CRYSTAL GROWTH & DESIGN

Article

pubs.acs.org/crystal

Electrospray Crystallization for Nanosized Pharmaceuticals with Improved Properties

Norbert Radacsi,*[,†] Rita Ambrus,[‡] Tímea Szunyogh,[‡] Piroska Szabó-Révész,[‡] Andrzej Stankiewicz,[†] Antoine van der Heijden,[†,§] and Joop H. ter Horst[†]

[†]Process & Energy Laboratory, Delft University of Technology, Leeghwaterstraat 44, 2628 CA Delft, The Netherlands

[‡]Department of Pharmaceutical Technology, University of Szeged, Eötvös Street 6, H-6720 Szeged, Hungary

[§]Technical Sciences, TNO, 2280 AA Rijswijk, The Netherlands

Supporting Information

ABSTRACT: Many new pharmaceuticals have low water solubility, hampering their pharmaceutical activity upon administering. One approach to increase solution concentrations during drug administration is to increase the surface-to-volume ratio by decreasing the crystal product size. Sub-micrometer-sized niflumic acid crystals were produced by electrospray crystallization. Electrospray crystallization uses a high potential difference to create a mist of ultrafine charged solution droplets. The subsequent total solvent evaporation and droplet disruption process lead to crystallization of sub-micrometer-sized crystals. For concentrations well below the solubility concentration while using small nozzle diameters, niflumic acid crystals with a size of 200−800 nm were produced. In the absence of excipients, for the sub-micrometer-sized niflumic acid no significantly different dissolution profile compared to the conventional one was measured. However, if excipients were added, the dissolution rate for the sub-micrometer-sized product increases substantially in stimulated gastric juice, while that of the conventional product increased slightly. Probably the excipients avoid the aggregation of the hydrophobic sub-micrometer particles in the low pH environment.

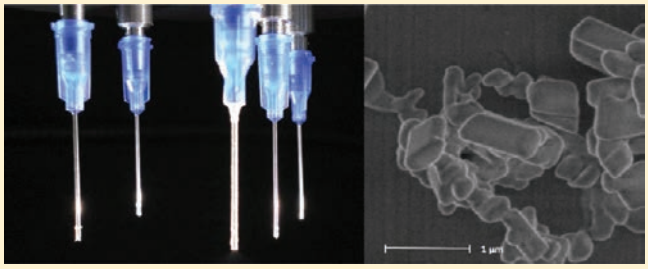

INTRODUCTION

The interest in sub-micrometer-sized particles has emerged both in industry and scientific research in the past decade.[1−3] Nano- and sub-micrometer-sized crystals may have different chemical and physical properties, because the particle surface properties dominate those of the particle volume. However, they can also have beneficial properties because of their small volume. Sub-micrometer-sized crystals are too small to contain inclusions of which the size is usually in the micrometer size range. It was shown previously that sub-micrometer-sized crystals have improved properties that indicate a higher internal quality (less inclusions and reduced dislocations) compared to conventionally sized particles of several tens to hundreds of micrometers.[4]

Since nearly half of the new active pharmaceutical ingredients (APIs) being identified are either insoluble or poorly soluble in water, solving bioavailability problems is a major challenge for the pharmaceutical industry.[5] Previously, the focus of this field was on the solution complexation[6] and amorphization[7] possibilities to increase the dissolution rate.[8−11] Since smaller particles have a much higher specific surface area, an increase in the dissolution rate (the amount of drug substance that dissolves per unit time) is expected at the same driving force for dissolution. An increase in the solubility might be expected as well, since according to the Ostwald−Freundlich relation, smaller particles have increased solubility.[12] However, an efficient, cost-effective, and simple technique to produce sub-micrometer particles of organic pharmaceutical compounds is still lacking.

Niflumic acid (NIF) is an important anti-inflammatory drug and also has a weak analgesic effect.[13] It is primarily used to treat different forms of rheumatism, such as rheumatoid arthritis or arthrosis, and to cure other inflammatory diseases.[14] However, its poor aqueous solubility[15] and dissolution rate[16] are disadvantages. To achieve optimal pharmacodynamic properties such as a rapid onset of the drug effect, fast dissolution is important for this type of drug.

Our aim is therefore to prepare sub-micrometer-sized NIF crystals in order to achieve fast dissolution. We introduce electrospray crystallization as a potentially efficient, cost-effective, and simple method for the production of such sub-micrometer-sized NIF crystals. The changes in dissolution profile as well as the product morphology and structural properties of the produced crystals are investigated in this paper.

Received: February 27, 2012
Revised: May 2, 2012
Published: May 18, 2012

ACS Publications © 2012 American Chemical Society

dx.doi.org/10.1021/cg300285w | *Cryst. Growth Des.* 2012, 12, 3514−3520

EXPERIMENTAL SECTION

Materials. Niflumic acid (2-[[3-(trifluoromethyl)phenyl]amino]-3-pyridinecarboxylic acid) with a mean size of around 80 μm (G. Richter Pharmaceutical Factory, Budapest, Hungary (see Figure S1 for SEM image of the manufacturer niflumic acid crystals (Supporting Information))), β-D-Mannitol (Hungaropharma Plc., Budapest, Hungary), and Poloxamer 188 (polyethylene-polypropylene glycol, Fluka, Ljubljana, Slovenia) were used as received. For the electrospray crystallization process, different solution concentrations were prepared with 99.8% acetone purchased from Merck. During the experiments, only acetone was used as a solvent, and thus the solvent effects were not investigated. Care was taken to choose materials in the device that withstand the exposure to acetone.

Single Nozzle Electrospray Crystallization Setup. The single nozzle electrospray crystallization setup was used to investigate the effect of the operating conditions and process parameters. This setup

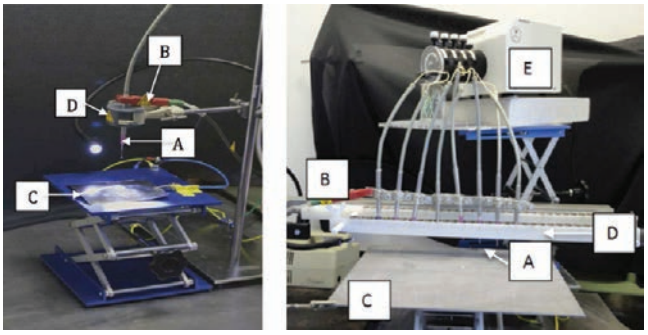

Figure 1. The single nozzle electrospray crystallization setup on the left and the eight-nozzle experimental setup on the right showing the capillary nozzle (A), high voltage connector (B), metal plate on which the particles are collected (C), the nozzle holder (D), and the Meredos TL-EAD peristaltic pump (E).

(see Figure 1) consisted of an Aitecs SEP-10S Syringe Pump with a 50 mL plastic syringe. A Wallis ±10 kV DC power supply was used in positive DC mode to provide the potential difference ΔU between the tip of the nozzle and the grounded plate, which were separated at a working distance D. The pump and a Festo 6 × 1 pneumatic tube were used to transport the solution with concentration c to the nozzle with a certain flow rate φ. Nozzles (EFD, USA) with a length of 25.4 mm varied in the inner diameter d (0.1524, 0.254, 0.3302, 0.4064, 0.508, 0.5842, and 1.3716 mm, referred to in the paper as respectively the 0.15, 0.25, 0.33, 0.4, 0.51, 0.58, and 1.37 mm nozzle for convenience). It was visually checked whether the electrospray setup was operated in cone-jet mode at specific sets of process parameters.

Multiple Nozzle Electrospray Crystallization Setup. The use of multiple nozzle setup has the advantage of higher production rates. An eight-nozzle system was used with a Meredos TL-EAD peristaltic pump in order to have an equal distribution of the solution flow over the nozzles (Figure 1). Otherwise the setup was similar to the single nozzle setup.

Characterization of the Product. For morphological and size characterization of the crystalline samples a Philips XL30 FEG and a FEI Nova NanoSEM 650 scanning electron microscopes (SEM) were applied. Typical settings of the instrument were 1−2 kV electron beam and 3−10 mm working distance. The samples were investigated without applying a conductive coating. A relatively low acceleration voltage was used in order to prevent extensive charging of the particles.

Differential scanning calorimetry (DSC) was employed to investigate the melting behavior of the NIF samples and the crystallinity as well. A thermal analysis system with the STAR^e thermal analysis program V9.1 (Mettler Inc., Schwerzenbach, Switzerland) was applied to characterize the thermal behavior of the products. The DSC measurements were done with 2−5 mg of NIF in the temperature range between 25 and 300 °C. The heating rate was 5 °C min^{-1}. Argon was used as carrier gas at a flow rate of 10 L h^{-1} during the DSC investigation.

X-ray diffraction (XRD) was carried out in order to determine the crystalline form of the produced materials and to examine the transition between amorphous and crystalline phase. Samples were measured with a Bruker D8 Advance diffractometer. The XRD patterns were recorded in Bragg−Brentano geometry. Data collection was carried out at room temperature using monochromatic Cu Kα1 radiation (λ = 0.154060 nm) in the 2θ region between 10° and 120°, step size 0.02 degrees 2θ. The sample of about 10 mg was directly deposited on a zero background holder (Si single crystal ⟨510⟩ wafer) and placed into the XRD directly after production. The record program of the pattern was relatively fast; it lasted for 160 s. Diffraction patterns were recorded 5, 20, and 75 min after production. Data evaluation was done with the Bruker program "EVA".

Solubility and Dissolution Rate Measurements. The solubility measurements were performed in a phosphate buffer solution (pH 1.2 ± 0.1) at 37 ± 0.5 °C. Twenty-five milligrams of NIF was dispersed in 5 mL of medium and stirred for 12 h at 37 °C. After filtration the dissolved drug amount in the medium was determined spectrophotometrically by an ATI-Unicam UV2-100 UV/vis spectrophotometer.

The dissolution profile of product samples containing equal amounts of drug (14 mg of NIF according to its therapeutic dose) was determined according to the paddle method.[17] A phosphate buffer solution (50 mL, pH 1.2 ± 0.1) at 37 ± 0.5 °C was used as a dissolution medium and the rotation speed of the paddles was 100 rpm. At time intervals, 2 mL solution samples were withdrawn and filtered (cutoff 0.2 μm, Minisart SRP 25, Sartorius, Germany), and the amount of dissolved drug was determined spectrophotometrically by an ATI-Unicam UV2-100 UV/vis spectrophotometer. It is common practice to replace the withdrawn samples with fresh medium. Dissolution behavior was determined in the presence and absence of excipients both for conventional and sub-micrometer-sized NIF. D-Mannitol and Poloxamer 188 were used as excipients to help the deaggregation and increase the wettability of the NIF crystals. D-Mannitol acts as a carrier, which provides the homogeneous distribution of the NIF crystals, while Poloxamer 188 helps as a stabilizer by wetting to arrest the aggregation of the drug. Table 1 shows the ratio of the excipients added to the drug. The physical mixtures were prepared using a Turbula mixer for 10 min as suggested by the manufacturer (Willy A. Bachofen Machinenfabrik, Switzerland). A homogeneous distribution of the NIF and the excipients was achieved by this mixing method without kneading or hard mechanical effects.

Table 1. The Ratio of the Niflumic Acid (NIF) and the Additives in the Samples Based on Weight

product	NIF	mannitol	Poloxamer
conventional NIF	1		
conventional NIF with excipients	1	2.5	0.25
sub-micrometer-sized NIF	1		
sub-micrometer-sized NIF with excipients	1	2.5	0.25

RESULTS AND DISCUSSION

First, the electrospray crystallization process parameters are investigated for operation in a cone-jet mode. Next, the process parameters for the desired submicrometer product are determined using the single nozzle electrospray setup. In the last part we characterize the product and determine its dissolution profile.

Electrospray Crystallization. To exploit the relations between the process parameters and the crystalline product quality (e.g., size), we need to understand the crystallization process during electrospray crystallization (Figure 2). A

dx.doi.org/10.1021/cg300285w | Cryst. Growth Des. 2012, 12, 3514−3520

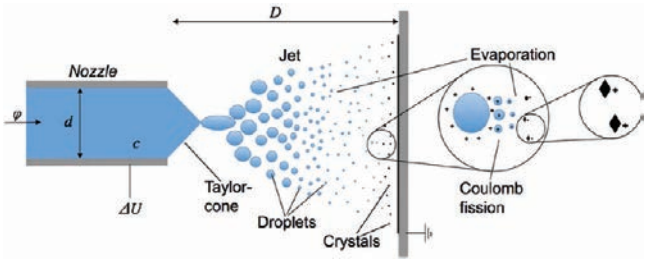

Figure 2. Schematic representation of the electrospray crystallization. Using a small nozzle diameter (d), a low constant flow rate (φ), relatively low solute concentration (c) a jet of highly charged small droplets will be emitted from the appeared cone at the nozzle tip upon a high enough potential difference (ΔU) is applied at a certain working distance (D). During the time the droplets are traveling to the grounded plate solvent evaporation and Coulomb fission occur leading to nucleation and crystal growth.

constant potential difference is applied between a grounded plate and a metal capillary (the nozzle), through which a conductive solution is pumped at a certain flow rate. If the potential difference is sufficiently high, electrostatic forces overcome the surface tension and a jet of liquid is emitted from the Taylor cone, formed at the nozzle.[18] After some distance from the nozzle, the jet becomes unstable and breaks into droplets, which are accelerated toward the grounded plate by the electric field. Because of the potential difference and the use of a conducting solution the surface of the droplets is charged. The surface charge density is mainly determined by the potential difference, the conductivity of the solution, and the nozzle diameter. Coalescence of droplets is prevented because of the unipolar charge,[19] which is important for preventing agglomeration and enables production of sub-micrometer crystals. Upon using a sufficiently volatile solvent such as acetone, solvent evaporation from the droplet occurs, which increases the surface charge density because of the decrease in droplet volume and area. As the surface charge reaches a critical value (Rayleigh limit[20]) electrostatic forces overcome the surface tension and the droplet disrupts into smaller droplets to reduce the surface charge density by creating more surface area. This disruption process is called Coulomb fission.[21]

There are different operating modes of electrospray process depending on the potential difference and flow rate. When operated in the cone-jet mode, a stable jet is developed that consists of highly charged small solution droplets, from which monodisperse, and sub-micrometer-sized particles can be formed.[22]

The solute concentration increases as the solvent evaporates from the droplet. At some point during this process of droplet evaporation and disruption, the driving force for crystallization becomes sufficiently large for crystal nucleation and growth to occur. The micrometer-sized droplets contain a small quantity of solute, so the produced crystals are in the sub-micrometer range. Thus, sub-micrometer- or even nanosized crystals can be formed upon total evaporation of the solvent. Aggregation of formed crystals during spraying is prevented since the crystals also have charges of equal sign. These charged sub-micrometer crystals accumulate at the grounded surface where they lose their surface charge.

Five exploitable process parameters were identified for this study: nozzle diameter (d), flow rate (φ), potential difference (ΔU), initial solute concentration (c), and working distance (D - the distance between the nozzle tip and the grounded plate). All the experiments were performed with solutions at room temperature, but the temperature of droplets in the jet could be lower due to the cooling effect of the evaporation of the acetone.

Effect of Process Parameters on Jet formation. The first step was to find the process parameters for the cone-jet mode. For this purpose the single nozzle electrospray setup was used. The solubility of NIF in acetone was determined to be approximately 110 mg mL^{-1} at room temperature. Solute concentrations close to the solubility caused nozzle blockage by the encrustation of crystals on the nozzle tip. Therefore, a low NIF concentration (20 mg mL^{-1}) was used.

Cone-jet mode is established if a stationary droplet emission from the nozzle takes place. This is a function of the nozzle diameter d, working distance D, flow rate φ, the potential difference ΔU, and the solution properties (conductivity, surface tension, and solute concentration c). There is a minimum threshold potential difference for establishing cone-jet mode (Figure 3). For example, using a NIF concentration of

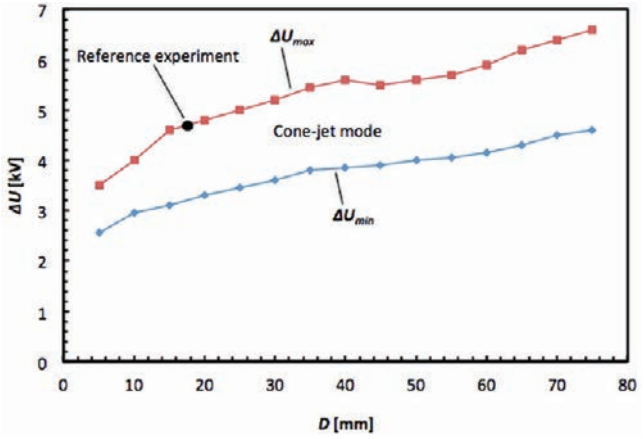

Figure 3. The minimum (ΔU_{min}) and maximum potential difference (ΔU_{max}) at different working distances to obtain a cone-jet mode using a NIF concentration of 20 mg mL^{-1} in acetone, a nozzle diameter of 0.33 mm, and a flow rate of 1.8 mL h^{-1}. Above the upper line multiple jets were obtained, and below the lower line no jet or intermittent cone-jet mode was observed. The black point represents the reference experiment.

20 mg mL^{-1} in acetone, a nozzle diameter of 0.33 mm, and a flow rate of 1.8 mL h^{-1}, a minimum potential difference of 3.3 kV is needed to enter the cone-jet mode at 20 mm working distance. Below that threshold no jet or only an intermittent jet was formed.

Above the minimum threshold voltage, a single continuous jet is formed (cone-jet mode) up to a certain maximum threshold potential difference (+4.8 kV using of 20 mg mL^{-1} solution concentration in acetone, a nozzle diameter of 0.33 mm and a flow rate of 1.8 mL h^{-1} and 20 mm working distance). Above this maximum threshold, multiple Taylor-cones are formed due to the large surface charge density at the nozzle tip, and with it multiple jets are formed, each originating from an individual Taylor-cone.

Figure 3 shows the minimum and maximum potential difference, ΔU_{min} and ΔU_{max}, for obtaining a continuous, single jet as a function of the working distances using a NIF solution concentration of 20 mg mL^{-1}, a flow rate of 1.8 mL h^{-1}, and a nozzle diameter of 0.33 mm. The width of the cone-jet mode operation window increased with the working distance. At 10

dx.doi.org/10.1021/cg300285w | Cryst. Growth Des. 2012, 12, 3514−3520

mm working distance, the operation window was around 1 kV wide, while at a working distance of 20 and 75 mm a width of respectively 1.5 and 2 kV was observed.

The solution flow rate also effects the jet formation. At a potential difference of +4.7 kV and a working distance of 17 mm a stable, single jet was observed only with a flow rate between 1.8 and 2.2 mL h^{-1}. It seems that only a very small operation window for the flow rate exists in electrospray crystallization of NIF from acetone.

Figure 4 shows the relation between nozzle diameter d and potential difference ΔU using a NIF concentration of 20 mg

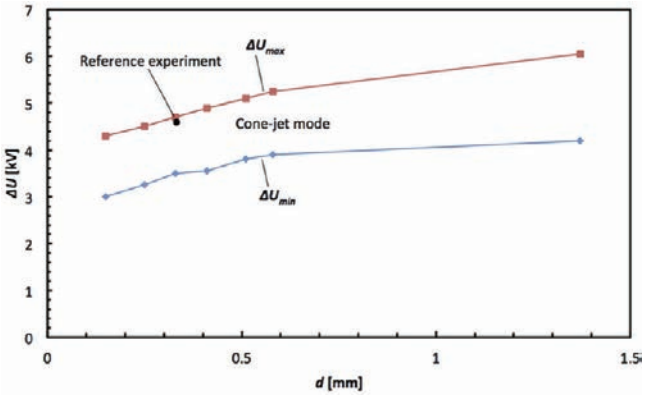

Figure 4. The minimum (ΔU_{min}) and maximum potential difference (ΔU_{max}) at different nozzle diameters to obtain a single jet using a concentration of 20 mg mL^{-1} NIF solution in acetone, a working distance of 17 mm, and a flow rate of 1.8 mL h^{-1}. Above the upper line multiple jets were obtained, and under the lower line no jets were obtained. Between the lines a single jet was obtained. The black point represents the reference experiment.

mL^{-1} in acetone at a working distance of 17 mm and a flow rate of 1.8 mL h^{-1} for cone-jet mode operation. A larger nozzle diameter demands a higher potential difference in order to obtain a continuous jet. At a larger nozzle diameter, the cone surface is larger, and thus, a higher potential difference is needed to overcome the increased total surface energy.[22] The width of the operation window for the potential difference to obtain a continuous jet was about 1.2−1.3 kV for all nozzle diameters used, except for the largest one, which was about 1.85 kV window for operation.

We can conclude that the process parameters need a strict balance to obtain a cone-jet mode. The operation window is quite narrow for establishing the cone-jet mode using NIF-acetone solutions.

Effect of Process Parameters on Particle Characteristics. Using a solution with a NIF concentration of 20 mg mL^{-1} the cone-jet mode was observed at a potential difference of +4.7 kV, a nozzle diameter of 0.33 mm, a working distance of 17 mm, and a flow rate of 1.8 mL h^{-1}. These process parameters were used to establish a reference experiment concerning product characteristics (Table 2).

The resulting sub-micrometer-sized crystals of the reference experiment are shown in Figure 5A. The produced crystals have a somewhat prismatic shape, while the size ranges from 200 to 800 nm and no extensive agglomeration is observed. Under these conditions, very small droplets are formed during the process and the small droplet volume causes the nucleation and growth of only a single NIF crystal per droplet. However, after the crystals were collected from the grounded plate into a Petri

Table 2. The Process Parameters for the Reference Electrospray Crystallization Experiment for NIF: Potential Difference (ΔU), Working Distance (D), Nozzle Diameter (d), Concentration (c), and Flow Rate (φ)[a]

ΔU [kV]	D [mm]	c [mg mL^{-1}]	d [mm]	φ [mL h^{-1}]
+4.7	17	20	0.33	1.8

[a]Using these parameters a continuous jet is formed.

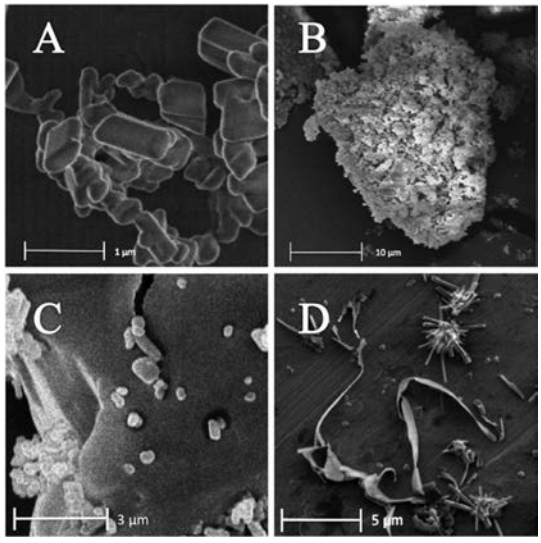

Figure 5. (A) 200−800 nm sized NIF produced in the reference electrospray crystallization experiment (see Table 1 for the process conditions). The SEM image shows the crystals directly deposited on the grounded plate. (B) A 30 μm NIF cluster created by the aggregation of the sub-micrometer-sized NIF crystals after removing the product from the grounded plate. (C) Aggregated and individual sub-micrometer-sized NIF crystals on the surface of D-mannitol after mixing. (D) Ribbon-shaped and agglomerated needle-like crystals of NIF and agglomerates produced using the 0.41 mm nozzle at a potential difference of +4 kV, a working distance of 17 mm, a solution concentration of 25 mg mL^{-1}, and a flow rate of 1.8 mL h^{-1}.

dish, sometimes the sub-micrometer-sized crystals aggregated into 20−30 μm sized clusters (Figure 5B), possibly due to the strong interactions between the hydrophobic crystal surfaces of these sub-micrometer-sized crystals. After mixing the sub-micrometer-sized NIF with the excipients, these agglomerates are partially or totally disintegrated, as can be seen in Figure 5C of the sub-micrometer-NIF on the surface of a D-mannitol crystal. This reference experiments shows that electrospray crystallization can be used to obtain sub-micrometer-sized crystals of NIF.

Three process parameters were identified in our system to have a major effect on the product size and tendency for agglomeration: solution concentration, potential difference, and the nozzle diameter. Higher potential difference or smaller nozzle diameter results in increased charge density of the droplets. Although it was reported that the flow rate also has significant effect on the product,[22] probably due to the narrow operation window for the flow rate, in our system no significant difference was observed when the flow rate was varied within this operation window.

Concentration. The solution concentration is a main parameter in determination of the final product. It was found that at higher initial concentrations the average crystal size increased: the same droplet with a higher concentration

dx.doi.org/10.1021/cg300285w | Cryst. Growth Des. 2012, 12, 3514−3520

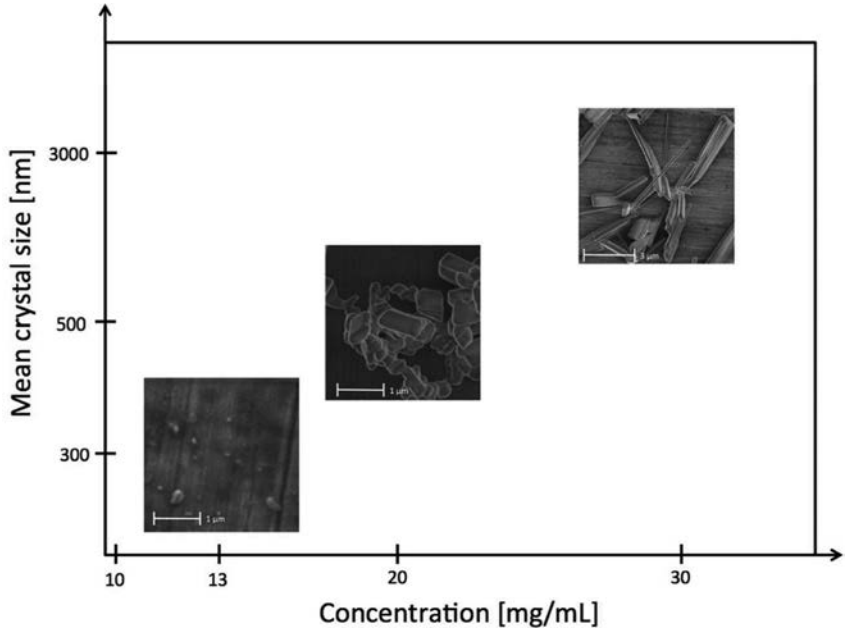

Figure 6. The relationship between the crystal size and shape and used solution concentration when NIF crystals are produced in electrospray crystallization. The crystal size increases with the increasing solution concentration, and the crystal shape becomes from somewhat spherical to needle-like.

contains more solute that can crystallize, resulting in larger crystals (Figure 6). This increasing size with increasing concentration coincides with previous findings of others.[23]

The crystal morphology also depends on the initial concentration. At higher concentrations the obtained crystals were more needle-like, while at lower concentrations the crystals had a somewhat spherical shape (Figure 6). At higher solution concentrations, crystallization occurs earlier after the droplets have left the nozzle. In our view the most probable explanation is that crystallization occurs even before Coulomb fission of the droplets, resulting in even larger crystals. At lower concentrations, crystallization occurs later, possibly after the Coulomb fission of the droplets.

When crystallized conventionally, in general NIF has a needle-like shape,[24] comparable to that in Figure 6 of an experiment at a higher concentration. The more compact and prismatically shaped crystals from the reference experiment indicate quite different growth behavior under these conditions.

Nozzle Diameter and Potential Difference. Figure 5D shows ribbon-shaped and agglomerated needle-like crystals produced in cone-jet mode using a larger nozzle diameter of 0.41 mm and lower potential difference of 4 kV compared to the reference experiment. As it was shown in Figure 4, the nozzle diameter and potential difference are coupled with each other. Lower potential difference or larger diameter of the nozzle results in a lower charge density at the Taylor-cone, and therefore, at the droplet surface. At a lower surface charge Coulomb-fission is occurring later or is absent and crystallization might occur in larger droplets, resulting in these ribbon-shaped and agglomerated needle-like crystals. The optimal concentration in our system for producing sub-micrometer-sized crystals with a compact and prismatic shape was found to be around 20 mg mL^{-1}, when the proper process conditions were applied.

Structure Analysis (DSC, XRD). The melting point of the sub-micrometer-sized drug was measured to be 199 °C, slightly lower than the original material (204 °C) and literature values[13] (see Figure S2 for DSC diagram (Supporting Information)). The lower melting point can be explained by the relatively large surface and thus increased total surface free energy compared to the original material.[25] The DSC results show that the normalized heat of melting for the electrosprayed material was 114 ± 6 J g^{-1}, 85% of that for the conventional NIF. This would indicate that the electrosprayed NIF is at least 85% crystalline.[26] XRD patterns of both the spherical and elongated NIF crystals did not indicate other crystalline forms than the single reported form.[24] Diffraction patterns recorded directly after spraying did not show remarkable change in time; however, the powder pattern at 75 min shows more and sharper peaks than the others, which could indicate a change in crystallinity in the measured time frame (see Figure S3 for XRD patterns (Supporting Information)). The product might be transformed during the production or in the short time frame between the experiment and the first analysis.

Solubility and Dissolution Rate Measurements. For measuring the solubility and dissolution rate 1.7 g of sub-micrometer-sized NIF crystals were produced using the reference experiment conditions in the eight-nozzle setup. The eight nozzle setup has under these conditions a production rate of 150 mg h^{-1} sub-micrometer-sized NIF.

Solubility and dissolution rate measurements of both the sub-micrometer-sized NIF and the raw material were performed. There were no significant differences measured between the solubility of the conventional (0.23 mg mL^{-1}) and the sub-micrometer-sized NIF samples (0.21 mg mL^{-1}). The sub-micrometer-sized and conventional NIF had also similar dissolution profiles at gastric pH. The explanation for this is that the nanoparticles tend to aggregate, and the advantage of the small size diminishes. The typical size of these aggregates was found to be around 30 μm (Figure 5B), which corresponds to the values found in the literature.[27] Therefore, both solubility and dissolution rate measurements were performed in the presence of the excipients D-mannitol and Poloxamer 188. These additives prevent aggregation of powders for both the

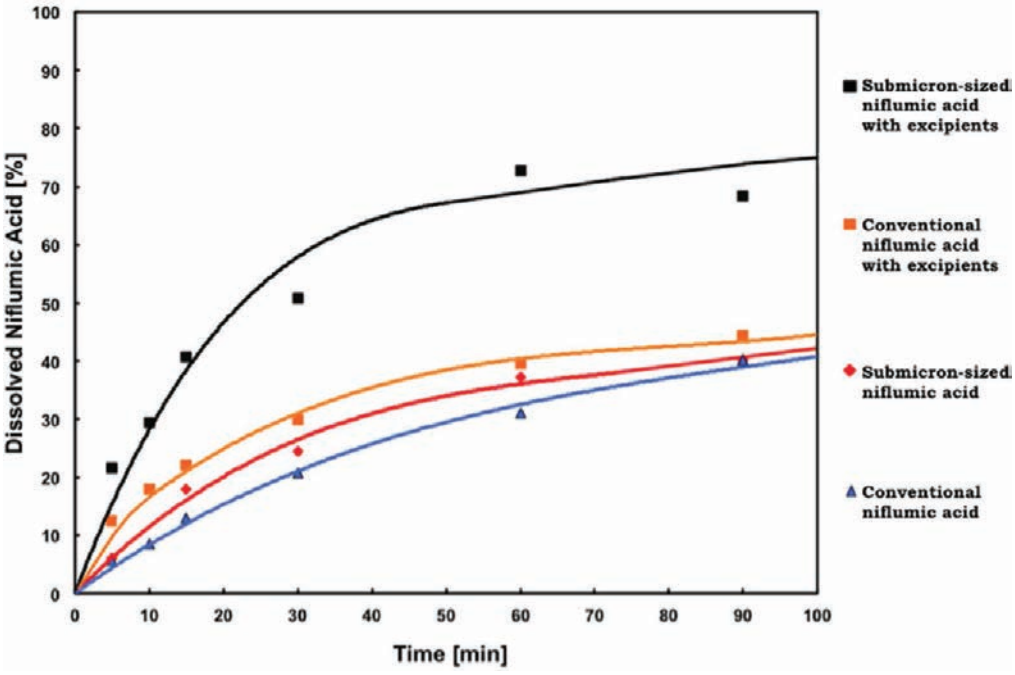

Figure 7. Dissolution profile of the conventional NIF without excipients (blue) and with excipients (orange) and the produced submicrometer-sized NIF without excipients (red) and with excipients (black). Using the conventional NIF with the excipient D-mannitol and Poloxamer 188 only 22% of the drug was dissolved after 15 min and 39% in 1 h. When the sub-micrometer-sized NIF was applied with the same excipients the dissolution increased to 41% after 15 min and 73% in 1 h.

conventional and sub-micrometer-sized NIF.[28,29] In the presence of the excipients the solubility of the sub-micrometer-sized NIF still did not increase. However, its dissolution profile changed significantly. Figure 7 shows the measured dissolution profile with and without the excipients added to the conventionally sized and sub-micrometer-sized NIF. In the presence of the excipients the measured dissolution profile of the conventional NIF was not significantly different. However, when using the sub-micrometer-sized NIF in the presence of the excipients, significantly higher dissolution rates were achieved. Using the conventional NIF with the excipient D-Mannitol and Poloxamer 188, only 29% of the drug was dissolved after 30 min. When the sub-micrometer-sized NIF was applied with the same excipients the dissolution increased to 51% in the same amount of time. It seems that preparation of sub-micrometer-sized NIF with excipients preventing aggregation results in higher drug dissolution rates and therefore an improved absorption is possible.

CONCLUSIONS

Sub-micrometer-sized niflumic acid crystals in the 200−800 nm size range can be produced by electrospray crystallization. However, the operation window for producing crystals in sub-micrometer range without extensive agglomerations or ribbon formation is rather small. High solution concentrations in combination with large nozzle diameter resulted in ribbon-shaped and agglomerated needle-like crystals having the same crystal structure. When the excipients D-mannitol and Poloxamer 188 were mixed with the sub-micrometer-sized niflumic acid the dissolution rate of the drug was enhanced. We can conclude that it is possible to increase the bioavailability of drugs by drastically reducing the crystal size of niflumic acid, while preventing their aggregation by applying the proper excipients.

ASSOCIATED CONTENT

Supporting Information

SEM image of the niflumic acid crystals, obtained from the manufacturer, DSC spectra of the sub-micrometer-sized niflumic acid compared with the original sample, and XRD patterns of the produced crystals made after the production are available. This material is available free of charge via the Internet at http://pubs.acs.org.

AUTHOR INFORMATION

Corresponding Author

*E-mail: n.radacsi@tudelft.nl.

Notes

The authors declare no competing financial interest.

ACKNOWLEDGMENTS

The authors thank Caner Yurteri for the introduction to electrospray and technical discussions on it, Yves Creyghton for providing the laboratory and equipment, and Ilse Tuinman for providing the peristaltic pump. Furthermore, the authors also thank Willem Duvalois, Ruud Hendrikx, and Emile van Veldhoven for the sample analysis and Dimo Kashchiev for interesting and helpful discussions. "TÁMOP-4.2.1/B-09/1/KONV-2010-0005. Creating the Center of Excellence at the University of Szeged" is supported by the European Union and cofinanced by the European Regional Development Fund.

REFERENCES

(1) Xu, Y.; Al-Salim, N.; Hodgkiss, J. M.; Tilley, R. D. *Cryst. Growth Des.* **2011**, *11*, 2721−2723.
(2) Naito, T.; Kakizaki, A.; Inabe, T.; Sakai, R.; Nishibori, E.; Sawa, H. *Cryst. Growth Des.* **2011**, *11*, 501−506.
(3) Kim, J.-W.; Shin, M.-S.; Kim, J.-K.; Kim, H.-S.; Koo, K.-K. *Ind. Eng. Chem. Res.* **2011**, *50*, 12186−12193.

(4) Radacsi, N.; Stankiewicz, A. I.; Creyghton, Y. L. M.; van der Heijden, A. E. D. M.; ter Horst, J. H. *Chem. Eng. Technol.* **2011**, *34*, 624−630.
(5) Saharan, V. A.; Kukkar, V; Kataria, M.; Gera, M; Choudhury, P. M. *Int. J. Health Res.* **2009**, *2*, 107−124.
(6) Kata, M.; Ambrus., R.; Aigner, Z. *J. Incl. Phenom* **2002**, *44*, 123−126.
(7) Ambrus, R.; Aigner, Z.; Soica, C.; Peev, C.; Szabó-Révész, P. *Rev. Chim.* **2007**, *58*, 206−209.
(8) Kesisoglou, F.; Panmai, S.; Wu, Y. *Adv. Drug Delivery Rev* **2007**, *59*, 631−644.
(9) Leuner, C.; Dressmann, J. *Eur. J. Pharm. Biopharm.* **2000**, *50*, 47−60.
(10) Rabinow, B. E. *Nat. Rev. Drug Discov.* **2004**, *3*, 785−796.
(11) Patravale, V. B.; Date, A. A.; Kulkarni, R. M. *J. Pharm. Pharmacol.* **2004**, *56*, 827−840.
(12) Müller, R. H.; Peters, K. *Int. J. Pharm.* **1998**, *160*, 229−237.
(13) *The Merck Index*, 11th ed.; Budavari, S.; O'Neil, M. J., Smith, A., Heckelman, P. E., Eds.; Merck & Co.: Rahway, NJ, 1989; Monograph 6444.
(14) *Martindale: The Extra Pharmacopoeia*, 31st ed.; Reynolds, J. E. F., Ed.; The Royal Pharmaceutical Society: London, 1996.
(15) Takács-Novák, K.; Avdeef, A.; Box, K. J.; Podányi, B.; Szász, Gy. *J. Pharm. Biomed. Anal.* **1994**, *12*, 1369−1377.
(16) Ambrus, R.; Aigner, Z.; Dehelean, C.; Szabó-Révész, P. *Rev. Chim.* **2007**, *58*, 60−64.
(17) *European Pharmacopoeia*, 3rd ed.; Council of Europe: Strasbourg, 1996; pp 128−129.
(18) Taylor, G. I. *Proc. R. Soc. London A* **1964**, *280*, 383.
(19) Yurteri, C. U.; Hartman, R. P. A.; Marijnissen, J. C. M. *Kona* **2010**, *28*, 91−115.
(20) Rayleigh, L. *Philos. Mag.* **1882**, *14*, 184−186.
(21) Suzuki, K.; Matsumoto, H.; Minagawa, M.; Kimura, M.; Tanioka, A. *Polym. J.* **2007**, *39* (11), 1128−1134.
(22) Hartman, R. P. A. *Electrohydrodynamic Atomization in the Cone-Jet Mode*. Ph.D. dissertation, Delft University of Technology: Delft, 1998.
(23) Scholten, E.; Dhamankar, H.; Bromberg, L.; Rutledge, G. C.; Hatton, T. A. *Langmuir* **2011**, *27*, 6683−6688.
(24) Krishna Murthy, H. M.; Vijayan, M. *Acta Crystallogr.* **1979**, *B35*, 262−263.
(25) Yang, G. C.; Nie, F. D.; Huang, H. *J. Energ. Mater.* **2007**, *25*, 35−47.
(26) Wagner, M. *Thermal Analysis in Practice;* Mettler-Toledo AG: Schwerzenbach, 2009; Chapter 7.6: DSC Evaluations, pp 90−132.
(27) van Ommen, J. R.; Yurteri, C. U.; Ellis, N.; Kelder, E. M. *Particuology* **2010**, *8*, 572−577.
(28) P. Kocbek, P.; Baumgartner, S.; Kristl, J. *Int. J. Pharm.* **2006**, *312*, 179−186.
(29) Hecq, J.; Deleers, M.; Fanara, D.; Vranckx, H.; Amighi, K. *Int. J. Pharm.* **2005**, *299*, 167−177.